Irrotational Subsonic Flow of an Ideal Gas in Two-Dimensional Ducts—Optimal Ducts and Ducts with Plane Sonic Exits

M. J. COHEN* AND H. PORTNOY*
Israel Institute of Technology, Haifa, Israel

A general series method of generating two-dimensional, inviscid, irrotational, compressible flows for ducts with a central plane of symmetry or with one plane wall is described, starting from a specified axial velocity distribution. By judicious choice of this distribution and selection of a suitable streamline as a boundary, two-dimensional, infinite duct shapes may be derived. A remarkable property of the solution enables us to specify a straight sonic line. It is demonstrated that the effects of series truncation and of actual physical truncation of the infinite portions of the duct may be kept within acceptable practical limits.

Nomenclature

$f_n(x)$ = coefficient in the series for ϕ; see Eq. (5)
$g_n(x)$ = coefficient in the series for $\log \bar{p}$; see Eq. (8)
i_j = typical member of a sequence of summation variables
j = summation variable
k = summation variable; also parameter in velocity distributions
m = summation variable
n = summation variable
p = summation variable; also fluid pressure
$\bar{p}$ = p/p_{oo}
s = variable used in Appendix 1
u = x-component of velocity divided by the fluid limiting velocity
v = y-component of velocity divided by the fluid limiting velocity
X = kx
x = coordinate measured parallel to the duct axis in the direction of flow from an arbitrary origin on the axis
x_o = value of x where flow becomes sonic
Y = ky
y = coordinate measured perpendicular to the flow, from an arbitrary origin on the axis of the duct
γ = ratio of specific heats of the fluid
ϕ = velocity potential; see Eq. (3)
$\phi_n(x)$ = envelope function for $|f_n(x)|$; see Sec. 8
ν = integer in the range 1 to n
ρ = fluid density
$\bar{\rho}$ = ρ/ρ_{oo}
τ = $(u^2+v^2)^{1/2}$
Δx = step length in numerical integration
$(\ )_o$ = subscript referring to conditions on the duct axis
$(\ )_{oo}$ = subscript referring to reservoir conditions
$(\ )_1$ = subscript referring to the starting point of the numerical integration procedure

1. Introduction

THE problem of converting an initially uniform fluid stream in a duct to a higher uniform velocity further downstream, while ensuring that the pressure variation along the wall of the duct is acceptable for boundary-layer control, is an important one particularly for wind-tunnel design. It is usually referred to as the "contraction" problem and the pressure is usually required to be monotonically decreasing as we proceed downstream along the wall, or at least regions of increasing pressure must be restricted and the rates of increase must be small in these regions.

The theoretical approach to this problem usually has been to treat the flow as inviscid axisymmetric or two-dimensional, since most wind-tunnel contractions approximate to one or the other of these geometries.

The axisymmetric incompressible case has been considered by Tsien,[1] Szczeniowski,[2] and Bloomer[3] who use as their starting point a specified distribution of velocity along the duct axis. This approach was extended by Cohen and Ritchie,[4] still in the incompressible case, and by Cohen and Nimery[5] for the case of axisymmetric compressible flow. A different approach to axisymmetric contraction design is that of Thwaites,[6] but this has so far been restricted to incompressible flows only.

Two-dimensional incompressible contraction design has been considered by Cheers,[7] Goldstein,[8] Lighthill,[9] Whitehead, Wu and Waters[10] and Mills.[11] The last paper is a two-dimensional version of Thwaites's work. For the case of a two-dimensional contraction with compressible flow, of particular importance in supersonic nozzle design, there has been a considerable amount of material published, some of the more important of which are listed in Refs. 12–16. Some of these, however, relate only to the supersonic case.

In Ref. 17, mention is made of a numerical solution to the problem of an axisymmetric convergent cone with a plane sonic exit obtained by Van Zhu Tsuan, but it appears that this method cannot be used to synthesise a plane sonic exit as part of a design requirement. Ovsiannikov[18] has shown that for two-dimensional jets exhausting from a reservoir into a space with sonic conditions, the sonic line across the jet is straight and at a finite distance from the outlet. He suggests that the free-boundary shape can be used to design the contraction part of a two-dimensional subsonic-supersonic nozzle so as to give the straight sonic line which is desirable as a starting point for the design of the supersonic effuser. However, the reservoir inlet conditions are impracticable to simulate in a duct flow and the constant pressure on the jet boundary is not ideal for boundary-layer control on a duct wall.

More recently, Hopkins and Hill[19] have investigated the effect of small throat radius of curvature on the transonic flow in an axisymmetric nozzle. The solution is based on a stipulated axial velocity distribution and takes the form of truncated power series for the geometric and dynamic flow properties in terms of the stream function. The sonic surface is nonplanar.

Norton[20] uses an elegant transformation method to obtain analytic solutions for axisymmetric, subsonic-supersonic nozzles. However, uniform flow is not achieved in the supersonic part because of the analytic nature of the solutions. Plane sonic throats are not dealt with.

Presented as Paper 72-08 at the 8th Congress of the ICAS, Amsterdam, The Netherlands, August 28–September 2, 1972; received June 6, 1973; revision received November 30, 1973. The authors wish to express their thanks to D. A. Nimery for writing the computer programs for the present work and for assistance in checking the lengthy algebraic development of the series coefficients.

Index categories: Hydrodynamics; Nozzle and Channel Flow; Subsonic and Transonic Flow.

* Associate Professor, Department of Aeronautical Engineering.

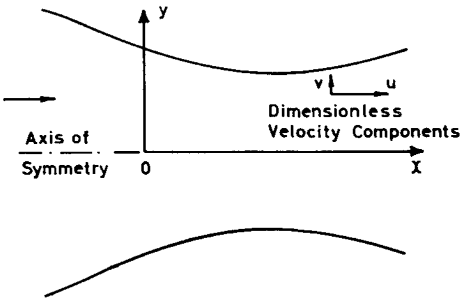

Fig. 1 Compressible flow in a two-dimensional duct with a central plane of symmetry.

Van Tuyl[21] starts from an assumed axial velocity distribution in the throat region and forms a Taylor series for the stream function. Padé functions are formed from the series to accelerate convergence. This analysis can be used to derive "short" convergent ducts in both two-dimensional and axisymmetric flow, but the possible occurrence of nonfavorable pressure gradients is not examined, nor is the question of a plane sonic surface dealt with.

Cohen and Nimery[22] have shown that, for axisymmetric ducts, their earlier work[5] can, in fact, be used to design contractions with subsonic inlet conditions and a specified sonic plane at the outlet section.

The present paper contains an extension of the work of Refs. 5 and 22 to two-dimensional ducts with a central plane of symmetry. A method of design exactly analogous to that of Ref. 5 is developed, starting from a specified axial velocity distribution, and it is demonstrated that a straight sonic line may be specified. A number of example designs are given and discussed. It should be noted that the present work applies unchanged to half nozzles obtained by replacing the central plane of symmetry by a solid wall, if boundary-layer effects are negligible or allowed for.

2. Fundamental Equations

Consider an ideal, irrotational, compressible flow in a two-dimensional duct with a central plane of symmetry, as shown in Fig. 1. The fluid is transformed from a uniform parallel flow at infinity upstream to a uniform parallel flow at infinity downstream. Axes are taken with origin O somewhere on the duct plane of symmetry, Ox along this plane of symmetry in the flow direction and Oy vertically upwards. The fluid pressure and density are p and ρ, respectively, u and v are velocity components parallel to Ox and Oy, respectively, rendered nondimensional by division by the limiting velocity of the fluid and $\tau = (u^2+v^2)^{1/2}$, the total dimensionless velocity magnitude.

If subscript oo refers to reservoir conditions, we define in addition

$$\bar{p} = p/p_{oo}, \qquad \bar{\rho} = \rho/\rho_{oo}$$

The equations of mass and energy conservation may now be written, respectively, as

$$[\partial(\bar{\rho}u)/\partial x] + [\partial(\bar{\rho}v)/\partial y] = 0 \tag{1}$$

and

$$\tau^2 + (\bar{p}/\bar{\rho}) = 1 \tag{2}$$

The requirement for irrotationality means that we can define a velocity potential ϕ such that

$$u = \partial\phi/\partial x, \qquad v = \partial\phi/\partial y \tag{3}$$

and since the flow is homentropic

$$\bar{p}/\bar{\rho}^{\gamma} = 1 \tag{4}$$

3. Series Expansions

We now assume a series for ϕ, having the required symmetry properties about the central plane. This is

$$\phi = \sum_{n=0}^{\infty} f_n(x) y^{2n} \tag{5}$$

Using Eq. (3), and denoting differentiation with respect to x by a dash, we get

$$u = \sum_{n=0}^{\infty} f_n'(x) y^{2n} \tag{6a}$$

$$v = 2\sum_{n=1}^{\infty} n f_n(x) y^{2n-1} = 2y \sum_{n=0}^{\infty} (n+1) f_{n+1}(x) y^{2n} \tag{6b}$$

The following derivatives are also required

$$\frac{\partial u}{\partial x} = \sum_{n=0}^{\infty} f_n''(x) y^{2n} \tag{7a}$$

$$\frac{\partial v}{\partial y} = 2\sum_{n=1}^{\infty} n(2n-1) f_n(x) y^{2n-2}$$

$$= 2\sum_{n=0}^{\infty} (n+1)(2n+1) f_{n+1}(x) y^{2n} \tag{7b}$$

Writing suffix o to refer to conditions on the plane of symmetry we may assume the following expansion for $\bar{\rho}$, having the required symmetry about $y = 0$

$$\bar{\rho} = \bar{\rho}_o(x) \exp\left\{\sum_{n=1}^{\infty} g_n(x) y^{2n}\right\} \tag{8}$$

and from Eq. (4) it follows that

$$\bar{p} = \bar{p}_o(x) \exp\left\{\gamma \sum_{n=1}^{\infty} g_n(x) y^{2n}\right\} \tag{9}$$

and

$$\frac{\bar{p}}{\bar{\rho}} = \frac{\bar{p}_o}{\bar{\rho}_o} \exp\left\{(\gamma-1) \sum_{n=1}^{\infty} g_n(x) y^{2n}\right\}$$

$$= (1-\tau_o^2) \exp\left\{(\gamma-1) \sum_{n=1}^{\infty} g_n(x) y^{2n}\right\} \tag{10}$$

where Eq. (2) has been used on the axis of symmetry.

In Appendix 1 it is shown that Eq. (10) can be expanded as

$$\frac{\bar{p}}{\bar{\rho}} = (1-\tau_o^2)\left\{1 + (\gamma-1)\sum_{n=1}^{\infty} (g_n + G_{n-1}[g]) y^{2n}\right\} \tag{11a}$$

where

$$G_{n-1}[g] = \sum_{j=1}^{n-1} (\gamma-1)^j \sum_{i_1=j}^{i_o-1} \sum_{i_2=j-1}^{i_1-1} \cdots \sum_{i_j=1}^{i_{j-1}-1} \left[\frac{(i_o-i_1)(i_1-i_2)\cdots(i_{j-1}-i_j)}{i_o i_1 i_2 \cdots i_{j-1}} g_{i_o-i_1} g_{i_1-i_2} \cdots g_{i_{j-1}-i_j} g_{i_j}\right] \tag{11b}$$

and i_o is to be identified with n, whereas the value of $G_{n-1}[g]$ is taken as zero when $n = 1$.

We also require the derivatives of $\log \bar{\rho}$. From Eq. (8) these are

$$\frac{\partial \log \bar{\rho}}{\partial x} = \frac{1}{\bar{\rho}_o}\frac{\partial \bar{\rho}_o}{\partial x} + \sum_{n=1}^{\infty} g_n'(x) y^{2n} \tag{12a}$$

and

$$\frac{\partial \log \bar{\rho}}{\partial y} = 2y \sum_{n=1}^{\infty} n g_n(x) y^{2n-2} \tag{12b}$$

4. Recurrence Relationships

Two sets of recurrence relationships are now derived which form an interlocking system from which the functions $f_n(x)$ and $g_n(x)$ may be found in terms of the specified distribution of velocity along the center line, τ_o.

If Eq. (1) is expanded and divided throughout by $\bar{\rho}$ we obtain

$$\frac{\partial u}{\partial x} + \frac{\partial v}{\partial y} + u\frac{\partial \log \bar{\rho}}{\partial x} + v\frac{\partial \log \bar{\rho}}{\partial y} = 0$$

Using Eqs. (6, 7, and 12) and at the same time changing summation variables as necessary to avoid confusion, we obtain

$$\sum_{n=0}^{\infty}\left[f_n''+2(n+1)(2n+1)f_{n+1}\right]y^{2n}+\sum_{n=0}^{\infty}f_n'y^{2n}\left[\frac{1}{\bar{\rho}_o}\frac{\partial\bar{\rho}_o}{\partial x}+\sum_{m=1}^{\infty}g_m'y^{2m}\right]+2y\sum_{n=0}^{\infty}(n+1)f_{n+1}y^{2n}\cdot 2y\sum_{m=1}^{\infty}mg_m y^{2m-2}=0$$

If the products of summations are replaced by double summations in which n is then replaced by $p-m$ we obtain, on reversing the order of these double summations and then replacing p by n

$$\sum_{n=0}^{\infty}\left[\frac{1}{\bar{\rho}_o}\frac{\partial}{\partial x}(\bar{\rho}_o f_n')+2(n+1)(2n+1)f_{n+1}\right]y^{2n}+\sum_{n=1}^{\infty}\sum_{m=1}^{n}\left[f_{n-m}'g_m'+4m(n-m+1)f_{n-m+1}g_m\right]y^{2n}=0 \tag{13}$$

Now Eqs. (2) and (4) applied on the axis yield

$$\bar{\rho}_o=(1-\tau_o^2)^{1/(\gamma-1)} \tag{14}$$

so that on substituting this in Eq. (13) together with $f_o'=\tau_o$, equation of the coefficients of like powers of y yields the following recurrence relationships:

$$f_1=\frac{(\gamma+1)\tau_o^2-\gamma+1}{2(\gamma-1)(1-\tau_o^2)}\tau_o' \tag{15a}$$

and

$$\underset{n>0}{f_{n+1}}=\frac{-1}{2(n+1)(2n+1)}\left\{f_n''-\frac{2f_n'\tau_o\tau_o'}{(\gamma-1)(1-\tau_o^2)}+\sum_{m=1}^{n}\left[f_{n-m}'g_m'+4m(n-m+1)f_{n-m+1}g_m\right]\right\} \tag{15b}$$

The second set of recurrence relationships is found by substituting Eqs. (11) and (6) into the energy equation (2), using the fact that $\tau^2=u^2+v^2$. We obtain

$$(1-\tau_o^2)\left\{1+(\gamma-1)\sum_{n=1}^{\infty}(g_n+G_{n-1}[g]y^{2n}\right\}=1-\left(\sum_{m=0}^{\infty}f_m'y^{2m}\right)^2-\left(2\sum_{m=1}^{\infty}mf_m y^{2m-1}\right)^2=1-f_o'^2-\sum_{n=1}^{\infty}\left\{f_n'f_o'+\sum_{m=1}^{n}(f_{n-m}'f_m'+4(n-m+1)mf_{n-m+1}f_m)\right\}y^{2n}$$

the last line being derived after a manipulation of the products of series similar to that described previously.

Equating coefficients of y^0 yields a result equivalent to

$$f_o'=\tau_o$$

Equating coefficients of y^{2n+2} gives the recurrence relationships

$$\underset{n>0}{g_{n+1}}=-\frac{\tau_o}{(\gamma-1)(1-\tau_o^2)}f_{n+1}'-\frac{1}{(\gamma-1)(1-\tau_o^2)}\sum_{m=1}^{n+1}\{f_{n+1-m}'f_m'+4(n+2-m)mf_{n+2-m}f_m\}-G_n[g] \tag{16}$$

The forms of the relationships (15) and (16) for $\gamma=1.4$ and $n=0$–3 are given in Appendix 2. These are the actual expressions used in the present work.

It is readily seen that Eqs. (15) and (16) form an interlocking set of relationships by means of which the functions f_n and g_n may be found, starting from the specified centerline velocity distribution τ_o. Thus, knowing τ_o, f_1 can be found from Eq. (15) and so g_1 can be found from the first of the set (16). Enough information is now available to calculate f_2 from Eq. (15), and so on. At each stage we switch to the next equation of the other set and can evaluate the right-hand side by substitution of functions already found, and their derivatives (of the first order for the g_n and up to the second order for the f_n).

Although this process is elementary, the algebra involved rapidly becomes very lengthy, so that the present work only carries the calculations up to and including the terms $f_4'y^8$ in u, $8f_4y^7$ in v and g_4y^8 in Eqs. (7–9). It is found nevertheless, that this number of terms gives an accuracy sufficient for practical purposes in all cases examined so far. This point, together with other aspects of accuracy, is discussed later on (see Sec. 8).

Each of the f_n, g_n, etc., which was calculated appears as a finite series of terms involving products of derivatives of τ_o multiplied by coefficients which are simple algebraic functions of τ_o (but which are, nevertheless, very lengthy expressions for the larger values of n). The results for a specific centerline velocity distribution τ_o are obtained by substitution in these general expressions.

5. Method of Duct Design

Once the f_n and g_n are found for a given centerline velocity distribution τ_o, the basic parameters of the associated flowfield can be computed from Eqs. (6, 8, and 9); other quantities derived from them, such as speed of sound and Mach number, can be also found.

This process may be used to design ducts to convert one uniform flow at infinity upstream into another uniform flow at infinity downstream. The duct must be doubly infinite, since τ_o has to be specified along the whole of the x-axis. However, by careful selection of τ_o, the flow may be effectively converted, for practical purposes, over a finite length of duct.

The procedure is as follows: after choosing a τ_o, u and v are found at the point $x=0$, $y=1$, using Eq. (6). Taking an increment Δx, the next point on the streamline through (0, 1) can be taken as being the point $(\Delta x, 1+(v/u)_1\Delta x)$ where subscript 1 refers to values at the first point (0, 1), and v and u can be found at this new point so that the slope v/u may be amended for the next increment. Proceeding in this way both upstream and downstream, the streamline through (0, 1) can be traced out together with its velocity distribution $(u^2+v^2)^{1/2}$. When the velocity differs from the value of τ_o at the same x, by an acceptable tolerance we conclude that the region of effectively uniform parallel flow has been reached and the numerical integration is stopped. Other streamlines may be similarly mapped starting at points such as (0, 0.8), (0, 1.2), and so on. Any one of the streamlines may be selected as a duct profile; the nearer the chosen streamline is to the axis, the more slender will the resulting contraction be and the fewer will be the number of terms of the series required. On the other hand, the further out the chosen boundary streamline is, the blunter will be the contraction, the more will be the number of terms of the series required for an acceptable accuracy [since we move further away from the one-dimensional flow, which is typified by the f_o' term in Eq. (6) only, with all other f and g functions vanishing] and the more will be the tendency for an adverse pressure gradient to occur on the wall. There will eventually be a streamline which just avoids adverse pressure gradients, which will represent the "optimal," bluntest contraction for the given τ_o, streamlines outside this one being unacceptable as duct shapes. It is, of course, possible that this selection of streamlines further and further out from the axis may be halted by the inadequacy of our truncated series before the optimal shape is reached, in which case this could only be found by extending the series further. However, in the cases so far computed, the number of terms specified previously has always proved adequate.

It should be emphasised that the optimal duct previously referred to is only optimal in the context of the specified τ_o distribution. It might be possible in any specific case to get a better optimal duct, i.e., a blunter, shorter one for the same velocity conversion by starting with a different τ_o distribution.

Matters connected with numerical accuracy, adequacy of the number of terms in the series, convergence tests, and so on, are discussed in Sec. 8 and the selection of τ_o distributions is discussed in Sec. 7.

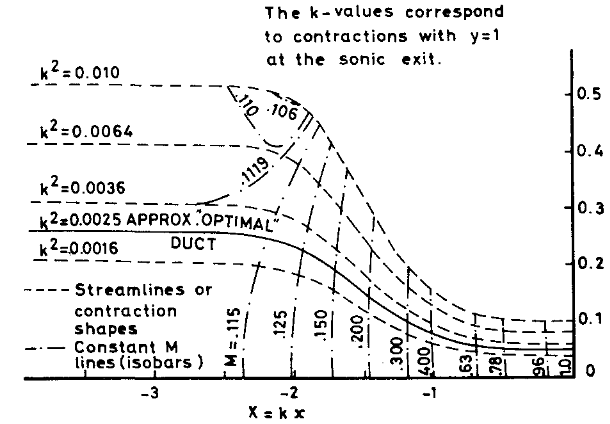

Fig. 2 Basic flow pattern.

6. Semi-Infinite Ducts with Sonic Outlets—Designing for a Plane Sonic Outlet

The method we have just described can be used for designing ducts with purely subsonic flow and is particularly suited to the design of contractions. These contractions will be infinite in extent in both the upstream and downstream directions as long as the delivery conditions downstream are subsonic.

However, in the particular case of SONIC delivery conditions the contraction can be made only semi-infinite, its sonic end occurring in the finite region, by a simple artifice; namely, to adopt an axial velocity distribution which accelerates to sonic conditions at some position $x = x_o$ along the duct axis and then decelerates to some subsonic value at infinity downstream. The subsonic DIFFUSER part of the nozzle is of no interest on physical grounds but once the flow has become sonic (even if immediately afterwards it decelerates to subsonic flow once more) the nozzle can be terminated at the sonic line to form a semi-infinite subsonic contraction with a sonic outlet. The sonic outlet flow may then be used as the starting point for designing a supersonic effuser by standard methods.

A very desirable condition at such a sonic outlet is that the sonic line should be straight and normal to the axis of symmetry. In Appendix 3 it is proved that if we select an axial velocity distribution with derivative τ_o' zero at the sonic point on the axis, such a straight sonic line, producing uniform sonic exit flow from the contraction cone, is automatically ensured. This remarkable property enables us to design contractions with plane sonic exists which are thus eminently suitable as the starting point for the supersonic effuser design.

7. Selection of Axial Velocity Distributions

The axial velocity distribution, τ_o, which is selected must be defined along the whole of the x-axis where all its derivatives must exist, and it must satisfy the conditions

$$\lim_{x\to\pm\infty} \frac{d^n\tau_o}{dx^n} = 0, \qquad n > 0 \tag{17}$$

In the case of infinite ducts, the value of τ_o must tend to the required inlet value as $x \to -\infty$ and to the required exit value as $x \to +\infty$.

For the semi-infinite ducts with sonic outlet, we may arbitrarily choose the outlet to be at $x = 0$ and the inlet at $x = -\infty$. The τ_o distribution must now have the required inlet value as $x \to -\infty$ and the value $1/(6)^{1/2}$ at $x = 0$, for diatomic gases. If the outlet is required to be a plane sonic surface we must also have $\tau_o'(0) = 0$. The τ_o distribution to the right of the exit need only be a bounded analytic continuation of the distribution to the left and it must, of course, satisfy condition (17).

In the present paper the following velocity distributions have been used to calculate examples.

1) Distribution A

$$\tau_o = 0.05 + \{[1/(6)^{1/2}] - 0.05\}\, e^{-k^2x^2} \tag{18}$$

with $k^2 = 0.0016, 0.0036, 0.0064$, and 0.01. The value of k^2 giving the bluntest cone without adverse gradients is also found.

This distribution converts a subsonic stream with value $\tau_o = 0.05$ at $-\infty$ to a uniform sonic flow across the line $x = 0$ and then returns it to $\tau_o = 0.05$ at $+\infty$. We are, of course, mainly interested in the left-hand half of the flow up to the plane sonic throat.

Since τ_o is a function of kx it is easily shown that the dimensionless velocity components, and hence the flow properties in general, are functions of

$$X = kx \quad \text{and} \quad Y = ky$$

only. Thus, when plotted in terms of X and Y the streamline patterns for different values of k become a single set of curves, which we may term the "basic flow pattern," and when plotted in this way, the optimal contractions for different values of k fall on a single curve.

The basic flow pattern is shown in Fig. 2 and the optimal cone is also shown there.

2) Distribution B

$$\tau_o = 0.05 + \{[1/(6)^{1/2}] - 0.05\}\, \mathrm{sech}^2\, kx \tag{19}$$

with $k = 0.04$, 0.08, 0.12, 0.16, and 0.2. Also, as before, the optimal value of k is found.

This distribution has the same over-all properties as Distribution A and the previous remarks hold for it too, including those concerning the basic flow pattern.

The results for the basic flow pattern are shown in Fig. 3.

8. Convergence and Accuracy of the Solutions

An examination of the complexity of the recurrence relationships in Sec. 4 shows that it is very unlikely that a formal proof of the convergence of the series expansions (6–8) is possible.

In the circumstances a numerical convergence check has been applied to the limited number of terms calculated, to provide at least some basis for the assumption of convergence.

The technique is based on a simple comparison test and is developed in Ref. 5. It may be briefly stated as follows: it has been found in all cases examined that the f_n and g_n appear to be oscillatory functions with damped amplitude as $x \to \infty$. The frequency increases and the maximum amplitude decreases with increasing n and it is reasonable to assume that these are general characteristics of the functions for velocity distributions such as we are interested in, even though they are only deduced from an inspection of the behavior of f_n and g_n for $n \leqq 4$ over a finite range of x for a limited number of τ_o. We are therefore able to define functions $\phi_n(x)$ to be envelopes of the $|f_n(x)|$ functions, and it is then shown in Ref. 5 that if the condition

$$[\phi_n(x)/\phi_{n-1}(x)]\, y^2(x) < 1$$

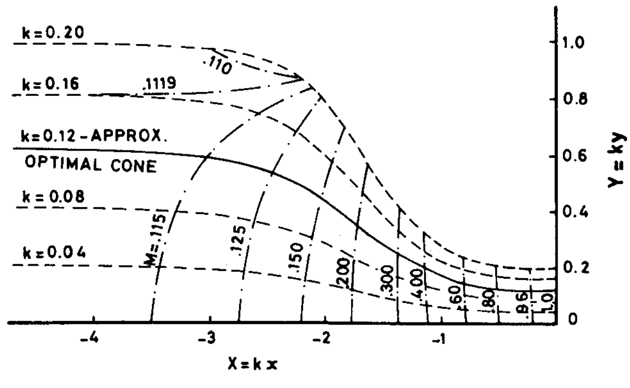

Fig. 3 Results for the basic flow pattern.

where $y(x)$ is the y-coordinate of the point at x for which the test is being applied, is satisfied for all n, then the series (5) is absolutely convergent for that value of x. The work in Ref. 5 refers, of course, to the axisymmetric case but the mathematical problem is the same, although a slight change of symbols is made here. In practice of course, we only apply this test for $n = 1, 2, 3$, and 4 at a finite number of discrete values of x. This does, however, enable us to approximately delineate the convergence boundary within the finite region examined, although it is not prudent in the circumstances to make use of streamlines, which approach this boundary too closely. A similar test is applied to the g_n to estimate the region of convergence of Eqs. (8–10).

The preceding test is reinforced by checking the mass flow at a number of values of x within the selected boundary streamline. This also serves as a check on the effects of truncating the series, and evidently we are limited in our ability to approach the convergence boundaries by the truncation error, which gets worse as we move out from the axis so that, in effect, we are forced to work well within this boundary. Errors in the mass flow at any station as compared with the known exact throat mass flow were kept to a maximum of 0.1% for $\Delta x = 0.001$, so that the duct ordinates are correct to the same percentage.

Another factor to be considered in assessing the accuracy is the effect of step length Δx. The calculations were done for $\Delta x = 0.01$ and $\Delta x = 0.001$ and the error in the ordinates calculated was reduced by an order of magnitude, i.e., from 1% to 0.1%, in the case of Distribution A.

The duct really extends to infinity at inlet (and outlet, if this is not taken at the sonic line). The infinite extension is assumed to be replaceable by a parallel channel beyond the point where the wall and axis velocities differ by less than 0.1%. This enables us to define the effective length of the varying portion of the duct or contraction and to define the slenderness ratio

$$\frac{\text{Total inlet height}}{\text{Effective length}}$$

where total height equals twice the value of y.

The optimal duct evidently has the largest slenderness ratio without adverse pressure gradients occurring on the wall, for the particular τ_o distribution selected.

9. Results and Discussion

The results of the preceding calculations are shown for Distribution A in Fig. 2 and for Distribution B in Fig. 3.

For Distribution A, the slenderness ratios obtained with $k^2 = 0.0016$, 0.0036, 0.0064 and 0.01 were, respectively, 1:6.74, 1:4.04, 1:3.48, and 1:2.8. The value of k^2 for the optimal duct was found to be 0.0025 and the corresponding slenderness ratio was 1:5.4.

Similarly for Distribution B the slenderness parameters corresponding to $k = 0.08$, 0.12, 0.16 are 1:5.9, 1:3.71, and 1:2 (estimated), respectively, and the optimal duct has $k = 0.12$ with a slenderness ratio 1:3.71.

Consideration of the flow pattern plots in Figs. 2 and 3 shows that the isobars (which can also be labelled as "iso-Mach Number" lines) seem to be showing a tendency to crowd together as they move upwards towards the line $M = 0.4$ where the iso-Mach-Number lines change their directions of curvature; those to the left being curved one way and those to the right, the other way. This line at about $M = 0.4$ seems to be straight and may be an asymptote for the other lines which crowd towards it.

Appendix 1

Consider the function

$$Q(s) = \exp\left\{(\gamma-1)\sum_{n=1}^{\infty} g_n s^n\right\} \tag{A1.1}$$

If Q can be expanded as

$$Q(s) = \sum_{n=0}^{\infty} h_n s^n \tag{A1.2}$$

we must have

$$h_o = Q(0) = 1 \tag{A1.3a}$$

$$h_n = \left(\frac{d^n Q}{ds^n}\right)_{s=0} \times \frac{1}{n!} \tag{A1.3b}$$

Now from Eq. (A1.1)

$$\log Q = (\gamma-1)\sum_{n=1}^{\infty} g_n s^n$$

$$\frac{dQ}{ds} = (\gamma-1)Q\sum_{n=1}^{\infty} n g_n s^{n-1}$$

Differentiating t times using Leibnitz's theorem

$$\frac{d^{t+1}Q}{ds^{t+1}} = (\gamma-1)\sum_{k=0}^{t}\frac{t!}{(t-k)!k!}\frac{d^kQ}{ds^k}\left(\frac{d}{ds}\right)^{t-k}\sum_{n=1}^{\infty} n g_n s^{n-1}$$

$$= (\gamma-1)\sum_{k=0}^{t}\frac{t!}{(t-k)!k!}\frac{d^kQ}{ds^k}\times \sum_{n=t-k+1}^{\infty}\frac{n!}{(n-t+k-1)!} g_n s^{n-t+k-1}$$

Putting $s = 0$ and using Eq. (A1.3)

$$\underset{t>0}{h_{t+1}} = \frac{\gamma-1}{(t+1)!}\sum_{k=0}^{t}\frac{t!}{(t-k)!k!}k!h_k(t-k+1)!g_{t-k+1}$$

$$= \frac{\gamma-1}{t+1}\sum_{k=0}^{t}(t-k+1)g_{t-k+1}h_k$$

This last expression is most conveniently expressed as

$$h_1 = (\gamma-1)g_1 \tag{A1.4a}$$

$$\underset{t\geq 1}{h_{t+1}} = (\gamma-1)g_{t+1} + \frac{\gamma-1}{t+1}\sum_{k=1}^{t}(t-k+1)g_{t-k+1}h_k \tag{A1.4b}$$

The solution of the recurrence equation (A1.4) may be effected as follows. If we define a function $G_n[g]$ by the statements

$$\underset{n\geq 1}{G_n}\,[g] = \sum_{j=1}^{n}(\gamma-1)^j\sum_{i_1=j}^{i_o-1}\sum_{i_2=j-1}^{i_1-1}\sum_{i_3=j-2}^{i_2-1}\cdots\sum_{i_j=1}^{i_{j-1}-1}\left[\frac{(i_o-i_1)(i_1-i_2)\cdots(i_{j-1}-i_j)}{i_o i_1 i_2\cdots i_{j-1}} g_{i_o-i_1}g_{i_1-i_2}\cdots g_{i_{j-1}-i_j}g_{i_j}\right] \tag{A1.5a}$$

where i_o is to be taken as $n+1$ and

$$G_o[g] \equiv 0 \tag{A1.5b}$$

then it is readily shown that

$$\underset{n\geq 1}{G_n}\,[g] = \frac{\gamma-1}{n+1}\sum_{k=1}^{n}(n-k+1)g_{n-k+1}(g_k + G_{k-1}[g]) \tag{A1.6}$$

It follows, therefore, that the solution of Eq. (A1.4) is

$$\underset{n\geq 1}{h_n} = (\gamma-1)(g_n + G_{n-1}[g]) \tag{A1.7}$$

so that the expansion of Eq. (A1.1) is

$$Q(s) = 1 + (\gamma-1)\sum_{n=1}^{\infty}(g_n + G_{n-1}[g])s^n \tag{A1.8}$$

which can be used to expand Eqs. (8–10).

Appendix 2

The expressions for $G_1[g]$, $G_2[g]$, etc., may be evaluated directly from the definition (A1.5) or by use of the recurrence relationship (A1.6). In either case we find

$$G_1[g] = [(\gamma-1)/2]g_1^{\,2} \tag{A2.1a}$$

$$G_2[g] = (\gamma-1)g_1g_2 + [(\gamma-1)^2/6]g_1^{\,3} \tag{A2.1b}$$

$$G_3[g] = (\gamma-1)(g_1g_3 + \tfrac{1}{2}g_2^{\,2}) + \frac{(\gamma-1)^2}{2}g_2g_1^{\,2} + \frac{(\gamma-1)^3}{24}g_1^{\,4} \tag{A2.1c}$$

etc.

We can now write down the two sets of recurrence relationships (15) and (16) for $n = 1, 2,$ and 3 and $\gamma = 1.4$.

We find from Eq. (15) (replacing f_o' by τ_o when it occurs)

$$f_1 = \frac{6\tau_o^2 - 1}{2(1-\tau_o^2)}\tau_o' \tag{A2.2a}$$

$$f_2 = -\frac{1}{12}\left(f_1'' - \frac{5\tau_o\tau_o'}{1-\tau_o^2}f_1' + \tau_o g_1' + 4f_1 g_1\right) \tag{A2.2b}$$

$$f_3 = -\frac{1}{30}\left(f_2'' - \frac{5\tau_o\tau_o'}{1-\tau_o^2}f_2' + f_1'g_1' + \tau_o g_2' + 8f_2 g_1 + 8f_1 g_2\right) \tag{A2.2c}$$

$$f_4 = -\frac{1}{56}\left(f_3'' - \frac{5\tau_o\tau_o'}{1-\tau_o^2}f_3' + f_2'g_1' + f_1'g_2' + \tau_o g_3' + 12f_3 g_1 + 16f_2 g_2 + 12f_1 g_3\right) \tag{A2.2d}$$

and from Eq. (16), using (A2.1) and again replacing f_o' by τ_o

$$g_1 = \frac{-5}{1-\tau_o^2}(2f_1^2 + \tau_o f_1') \tag{A2.3a}$$

$$g_2 = \frac{-5}{1-\tau_o^2}(\tfrac{1}{2}f_1'^2 + \tau_o f_2' + 8f_1 f_2) - \tfrac{1}{5}g_1^2 \tag{A2.3b}$$

$$g_3 = \frac{-5}{1-\tau_o^2}(\tau_o f_3' + f_1'f_2' + 8f_2^2 + 12f_1 f_3) - \tfrac{2}{5}g_1 g_2 - \tfrac{2}{75}g_1^3 \tag{A2.3c}$$

$$g_4 = \frac{-5}{1-\tau_o^2}(\tau_o f_4' + f_1'f_3' + 16f_1 f_4 + 24f_2 f_3 + \tfrac{1}{2}f_2'^2) - \tfrac{1}{5}g_2^2 - \tfrac{2}{5}g_1 g_3 - \tfrac{2}{25}g_1^2 g_2 - \tfrac{1}{375}g_1^4 \tag{A2.3d}$$

Appendix 3

Let us consider the sets of functions $f_n(x)$ and $g_n(x)$, which determine the flow, at a position $x = x_o$ where the flow is sonic, i.e.,

$$\tau_o(x_o) = [(\gamma-1)/(\gamma+1)]^{1/2} \tag{A3.1}$$

Let us suppose that it is stipulated that

$$\tau_o'(x_o) = 0 \tag{A3.2}$$

and that we have determined by inspection that under these conditions

$$f_\nu(x_o) = f_\nu'(x_o) = g_\nu(x_o) = g_\nu'(x_o) = 0, \quad 1 \leq \nu \leq n \tag{A3.3}$$

Using the recurrence relationships (15) together with Eqs. (A3.1, A3.2, and A3.3) it is now readily shown that

$$f_{n+1}(x_o) = \frac{-1}{2(n+1)(2n+1)}f_n''(x_o) \tag{A3.4}$$

$$f_{n+1}'(x_o) = \frac{-1}{2(n+1)(2n+1)}\left\{\left(\frac{\gamma-1}{\gamma+1}\right)^{1/2} g_n''(x_o) + f_n'''(x_o)\right\} \tag{A3.5}$$

and

$$f_{n+1}''(x_o) = \frac{-1}{2(n+1)(2n+1)}\left\{\left(\frac{\gamma-1}{\gamma+1}\right)^{1/2} g_n'''(x_o) + f_n^{iv}(x_o)\right\} \tag{A3.6}$$

Similarly, using Eq. (16) we can show that

$$g_{n+1}(x_o) = -[(\gamma+1)/(\gamma-1)]^{1/2} f_{n+1}'(x_o) \tag{A3.7}$$

$$g_{n+1}'(x_o) = -[(\gamma+1)/(\gamma-1)]^{1/2} f_{n+1}''(x_o) \tag{A3.8}$$

$$g_{n+1}''(x_o) = -[(\gamma+1)/(\gamma-1)]^{1/2} f_{n+1}'''(x_o) \tag{A3.9}$$

and

$$g_{n+1}'''(x_o) = -[(\gamma+1)/(\gamma-1)]^{1/2} f_{n+1}^{iv}(x_o) \tag{A3.10}$$

If we use Eq. (A3.8), with n in place of $n+1$ in Eq. (A3.4), we see that by virtue of Eq. (A3.3)

$$f_{n+1}(x_o) = 0 \tag{A3.11}$$

Using Eq. (A3.9) with n in place of $n+1$, Eq. (A3.5) becomes

$$f_{n+1}'(x_o) = 0 \tag{A3.12}$$

Similarly, using Eq. (A3.10), Eq. (A3.6) becomes

$$f_{n+1}''(x_o) = 0 \tag{A3.13}$$

so that by virtue of Eq. (A3.12), Eqs. (A3.13, A3.7, and A3.8) become, respectively,

$$g_{n+1}(x_o) = 0 \tag{A3.14}$$

and

$$g_{n+1}'(x_o) = 0 \tag{A3.15}$$

Since we can check that Eq. (A3.3) is true for $n = 1, 2,$ etc., by direct computation, it follows through Eqs. (A3.11, A3.12, A3.14, and A3.15), by induction, that

$$f_n(x_o) = f_n'(x_o) = g_n(x_o) = g_n'(x_o) = 0 \tag{A3.16}$$

for all $n \neq 0$.

It also follows from Eq. (A3.8) that

$$f_n''(x_o) = 0 \tag{A3.17}$$

for all n.

We have thus shown that if the axial distribution of velocity τ_o is chosen so that $\tau_o' = 0$ at the sonic position, then, by reference to Eqs. (5–10), there will be no variation of flow properties with y at that position and v will be zero, u will equal $[(\gamma-1)/(\gamma+1)]^{1/2}$ and $\partial u/\partial x$ will be zero across that section of the duct, i.e., a plane sonic surface (with $\partial u/\partial x = 0$ everywhere on it in addition) is obtained.

Finally, it should be remarked that for the axisymmetric duct solution,[5,22] the proof given previously applies in almost exactly the same form, since the second set of recurrence relationships (16) is the same in that case and the first set only differs slightly in the forms of the coefficients of the various terms; the differences being irrelevant to the preceding proof.

References

[1] Tsien, H. S., "On the Design of the Contraction Cone for a Wind Tunnel," *Journal of Aeronautical Science*, Vol. X, No. 2, 1943.

[2] Szczeniowski, B., "Contraction Cone for a Wind Tunnel," *Journal of Aeronautical Science*, Vol. X, No. 8, 1943.

[3] Bloomer, N. T., "Notes on the Mathematical Design of Nozzles and Wind-Tunnel Contractions," *Aeronautical Quarterly*, Vol. VIII, Aug. 1957.

[4] Cohen, M. J. and Ritchie, N. J. B., "Low-Speed Three-Dimensional Contraction Design," *Journal of the Royal Aeronautical Society*, Vol. 66, April 1962.

[5] Cohen, M. J. and Nimery, D. A., "Axisymmetric Nozzles for Compressible Flow," T.A.E. Rept. 122, April 1971, Technion—Israel Institute of Technology, Haifa, Israel.

[6] Thwaites, B., "On the Design of Contractions for Wind-Tunnels," R & M 2278, 1946, Aeronautical Research Council of Great Britain, London, England.

[7] Cheers, F., "Note on Wind-Tunnel Contractions," R & M 2137 1945, Aeronautical Research Council of Great Britain, London, England.

[8] Goldstein, S., "Notes on the Design of Converging Channels," R & M 2643, 1945, Aeronautical Research Council of Great Britain, London, England.

[9] Lighthill, M. J., "A New Method of Two-Dimensional Aerodynamic Design," R & M 2112, April 1945, Aeronautical Research Council of Great Britain, London, England.

[10] Whitehead, L. G., Wu, L. Y., and Waters, M. H. L., "Contracting Ducts of Finite Length," *Aeronautical Quarterly*, Vol. II, Feb. 1951.

[11] Mills, R. D., "Some Finite Two-Dimensional Contractions," *Aeronautical Quarterly*, Feb. 1968.

[12] Taylor, G. I., "The Flow of Air at High Speeds Past Curved Surfaces," R & M 1381, 1930, Aeronautical Research Council of Great Britain, London, England.

[13] Hooker, S. G., *Proceedings of the Royal Society, Ser. A*, Vol. 145, 1934.

[14] Lighthill, M. J., "The Hodograph Transformation in Transonic Flow," *Proceedings of the Royal Society, Ser. A*, Vol. 191, 1947.

[15] Fox, L. and Southwell, R. V., "On the Flow of Gas through a Nozzle with Velocities Exceeding the Speed of Sound," *Proceedings of the Royal Society, Ser. A*, Vol. 183, 1944.

[16] Binnie, A. M., "Notes on Gas Flow through a Nozzle," *Proceedings of the Cambridge Philosophical Society*, Vol. 46, 1950.

[17] Belotserkovski, R. M. and Chushkin, P. J., "A Numerical Method of Integral Relations," *Zhurnal Vych. Mat. i Mat. Fiz.*, Vol II,

1962; also *U.S.S.R. Computational Center for Mathematics and Mathematical Physics*, No. 5, Pergamon Press, New York, 1963.

[18] Ovsiannikov, L. V., "Gas Flow with Straight Transition Line," *Prikladnaya Matematicheskaia Mekhanika*, Vol. XIII, 1949; also TM 1295, May 1951, NACA.

[19] Hopkins, D. F. and Hill, D. E., "Effect of Small Radius of Curvature on Transonic Flow in Axisymmetric Nozzles," *AIAA Journal*, Vol. 4, No. 8, Aug. 1966, pp. 1337–1343.

[20] Norton, D. J., "Subsonic, Transonic, and Supersonic Nozzle Flow by the Inverse Technique," *Journal of Spacecraft and Rockets*, Vol. 9, No. 6, June 1972, pp. 457–459.

[21] van Tuyl, A. H., "Calculation of Nozzle Flows Using Padé Functions," *AIAA Journal*, Vol. 11, No. 4, April 1973, pp. 537–541.

[22] Cohen, M. J. and Nimery, D. A., "The Design of Axisymmetric Convergent Cones with Plane Sonic Outlets," *Israel Journal of Technology*, Vol. 10, No. 1–2, 1972, pp. 69–83.

MAY 1974 AIAA JOURNAL VOL. 12, NO. 5

Response of Separation to Impulsive Changes of Outer Flow

D. P. TELIONIS* AND D. T. TSAHALIS†
Virginia Polytechnic Institute and State University, Blacksburg, Va.

The unsteady boundary-layer equations are solved numerically for an impulsive change of the outer inviscid flow. The vanishing of the skin friction is not related to separation in unsteady flows and for this purpose an upwind differencing scheme is employed to integrate the boundary-layer equations through regions of partially reversed flow. The point of separation, as defined by Sears and Telionis, and the point of zero skin friction are plotted vs time. It is found that the point of zero skin friction jumps all the way to the leading edge immediately after the impulsive change of the outer flow and travels downstream for subsequent times. The point of separation instead remains at its original location, and only after some time elapses, it starts moving upstream. Both points asymptotically tend to the location of steady-state separation that corresponds to the new distribution of the outer flow.

Nomenclature

A = outer flow velocity gradient, see Eq. (16)
F = normalized longitudinal velocity component, $F = (u/U_e)$ at time t
F^0 = normalized longitudinal velocity component, $F^0 = (u/U_e)$ at time $t - \Delta t$
L = typical length of the problem
n = nondimensional distance normal to body surface
N = stretched normal coordinate, $N = n(Re)^{1/2}$
Re = Reynolds number
$S_u(t)$ = physical distance of unsteady separation point measured along the body surface from leading edge
$S_{zf}(t)$ = physical distance of the point of zero skin friction measured along the body surface from leading edge
s = nondimensional distance measured along the body surface from leading edge
t = time nondimensionalized with $\tau = (L/U_\infty)$
u = nondimensional viscous flow velocity component in s-direction
U = inviscid flow velocity component in s-direction
v = nondimensional viscous velocity component in n-direction
V = modified viscous velocity component in n-direction
α_j' = coefficients of the difference momentum equation for unsteady state, see Eq. (31)
α_j = coefficients of the difference momentum equation in the equivalent steady-state form, see Eq. (33)
β = pressure gradient parameter
η = transformed stretched normal coordinate
ξ = transformed surface coordinate

Subscripts

e = outer flow conditions
∞ = freestream conditions
H = initial steady-state solution

Received June 28, 1973; presented as Paper 73-684 at the AIAA 6th Fluid and Plasma Dynamics Conference, Palm Springs, Calif., July 16–18, 1973; revision received December 13, 1973. Research supported by the Air Force Office of Scientific Research, under Grant AFOSR-72-2361. The U.S. Government is authorized to reproduce and distribute reprints for Governmental purposes notwithstanding any copyright notation hereon.

Index categories: Boundary Layers and Convective Heat Transfer—Laminar; Nonsteady Aerodynamics.

* Assistant Professor, Engineering Science and Mechanics Department. Associate Member AIAA.

† Graduate Research Assistant, Engineering Science and Mechanics Department.

1. Introduction

THE importance of unsteady viscous flow problems has been widely recognized as reflected by the large number of recent publications on the topic.[1] Yet one of the characteristic features and a peculiar quirk of such flows, the phenomenon of separation, had not been properly defined more than 50 years after research in unsteady boundary layers was initiated. The location of actual separation regulates phenomena like the rotating stall in axial compressors or the stalling flutter of an air foil. This paper is definitely not the answer to all irksome questions on the topic. It provides though some encouraging indications that the research in this area is on the right path and supplies the results of calculations that could be easily reproduced experimentally for comparison.

For 60 years of research in boundary-layer theory, Prandtl's criterion[2] of vanishing skin friction has been used to predict effectively the phenomenon of separation. Only in the late fifties some concern was registered by Moore,[3] Rott[4] and Sears[5] about the validity of this criterion. It was then recognized that the classical criterion may lead to erroneous results in cases other than two-dimensional flow over fixed walls. Hartunian and Moore[6] have considered the case of a slowly moving point of separation. The similarity of the flow in the neighborhood of separation, for steady flow over fixed walls, was also pointed out. Vidal[7] and Ludwig[8] experimentally verified the theoretical models for steady flow over moving walls. Stewartson[9] used for